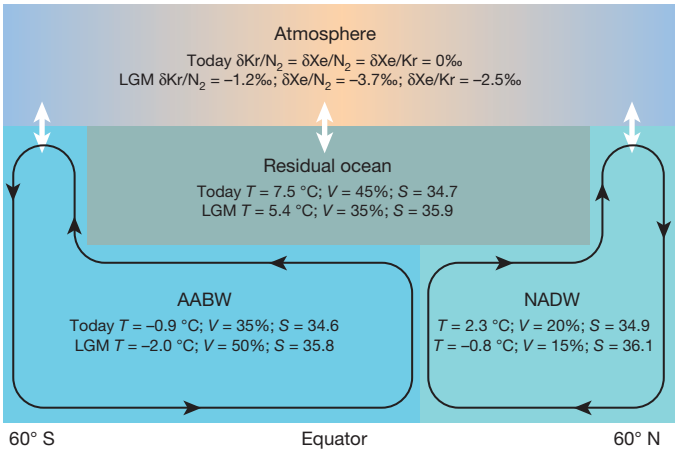

Figure 1 | Schematic of the four-box model used to derive MOT, including the modern ('Today') and LGM characteristics of the boxes. The shape and location of the boxes indicates roughly their zonally averaged situation in the modern ocean. Black arrows indicate the meridional circulation pattern of the two deep-water masses AABW and NADW. White arrows indicate the exchange of noble gases between the boxes and the geographical area in which they occur. The modern temperatures T, volumes V (as fraction of the total ocean) and salinities S (in units of the practical salinity scale, PSS) of AABW and NADW are based on ref. 20, while the parameters for the residual ocean are chosen such that the budget for the global average ocean ($T = 3.53$ °C; $S = 34.72$ PSS; $V = 100\%/1.34 \times 10^{18}$ m^3) is closed. The LGM parameters are based on the scaling of volume and salinity as well as the constraints from the noble gas data (see Methods for more details).

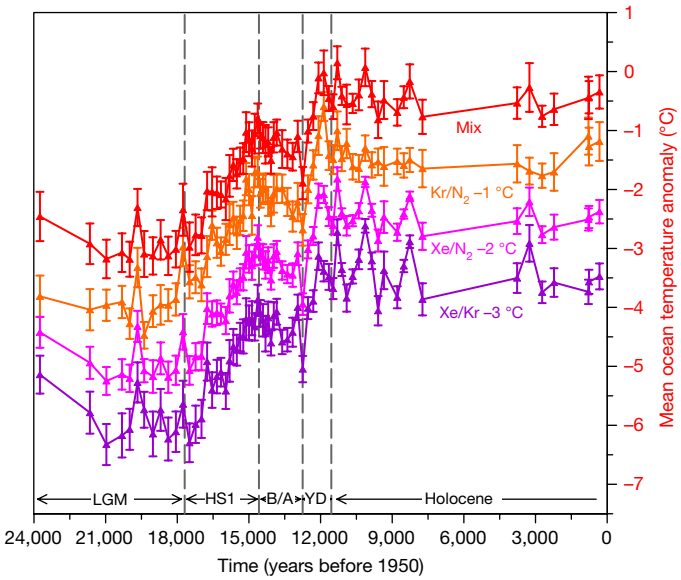

Figure 2 | MOT records relative to today derived from three different atmospheric noble gas ratios and their mixture. The records are based on 69 individual ice core samples with a distinct age (WD2014 age scale[36]), and each sample provides a separate value for atmospheric Kr/N_2, Xe/N_2 and Xe/Kr (if not subject to rejections; see Methods). Dashed vertical lines and labels mark different time periods (B/A, Bølling–Allerød; YD, Younger Dryas), as also in Fig. 3. The 'Mix' MOT record (red; best estimate) is not shifted, whereas the records based on the individual ratios are shifted as follows for better visibility: Kr/N_2 (orange) by −1 °C, Xe/N_2 (magenta) by −2 °C, Xe/Kr (purple) by −3 °C. Deviations of the individual records relative to each other are in Methods. The mean values and their error bars (1σ) include all analytical uncertainties and different scenarios as described in Methods.

The thermal fractionation correction is minor at the WAIS Divide ice core site owing to high accumulation rates and the gradual surface temperature changes[13], which limit the temperature differences over the length of the firn column to about 1 °C. The effects are, however, not negligible (approximately 0.25 °C change in MOT per 1 °C difference). Therefore, we correct our data for the thermal fractionation using two independent firn column temperature scenarios which represent the range of uncertainty of this correction element (see Methods). For our analysis below we combine the two scenarios in a Monte Carlo fashion to incorporate this uncertainty into our final best-estimate record.

To reconstruct MOT from the palaeo-atmospheric Kr/N_2, Xe/N_2 and Xe/Kr ratios, we use a four-box ocean–atmosphere model based on refs 9 and 10 (Fig. 1 and Methods). To account for changes in sea-level pressure, ocean volume and salinity, which affect the inventory of soluble gases in the ocean, we use the sea-level record of ref. 14. For each gas ratio 12,000 Monte Carlo MOT realizations are calculated that incorporate analytical uncertainties, uncertainties of the sea-level record, the degree of gas saturation, and those related to the applied firn thermal correction mentioned above (more details in Methods). We combine all realizations (36,000 in total) to a single best-estimate record (Fig. 2, red, 'Mix'). In this way, the obtained uncertainty accounts for inconsistencies between the estimated and effective thermal fractionation factors, for biases of the single-ratio MOT records (see Methods), as well as for all known model and analytical uncertainties. Thus, our uncertainty estimate is representative of the relative changes within our MOT record. Note that the uncertainty does not account for the potential bias induced by firn air disequilibrium mentioned above. Figure 3b shows a splined version of our best-estimate record with a low cut-off frequency so as not to dampen sharp features in our record; however, caution is required when interpreting excursions based on single data points, such as (for example) around 20 kyr BP.

Glacial–interglacial MOT difference

On the basis of our best-estimate record we determine the MOT change from the LGM to the Early Holocene (averaging periods marked by grey bars in Fig. 3) to 2.57 ± 0.24 °C (1σ). This is comparable to the estimates from marine proxies[4] of 3 ± 1 °C. The major contribution to the uncertainty estimate originates from a possible change in saturation state of the gases in the ocean. Today, the deep-water masses are slightly undersaturated with noble gases with respect to the water temperature[15,16]. During the LGM this undersaturation could have been reduced by about 50%, which would cause a bias in the LGM MOT of 0.24 °C in our best-estimate record (see Methods for more details). All other sources of uncertainty are of minor or negligible importance for this part of the analysis.

Even though MOT changes are related indirectly to average sea surface temperature (ASST) changes, which are in turn related to global average surface temperatures (GAST)—both important numbers for estimates of Earth system sensitivity[8,17–19]—it is not straightforward to constrain the LGM–Holocene ASST or GAST change from the MOT change we derive here. The main deep-water masses such as Antarctic Bottom Water (AABW) and North Atlantic Deep Water (NADW)—which represent today about 55% of the global ocean volume—are ventilated and thermally equilibrated in high-latitude areas[20,21] around 60°. Therefore, MOT is biased towards the polar regions in its representation of ASST. Furthermore, multiple lines of evidence suggest that the glacial deep water circulation was fundamentally different from today's, with a more stratified ocean and a larger AABW cell at the expense of the other water masses[22–25]. On the one hand, if one considers that surface temperature changes are amplified in higher latitudes compared to lower latitudes—a well known climate phenomenon known as polar amplification—one could argue that our LGM–Holocene MOT change represents an upper limit of average SST change. On the other hand, it is not clear by how much the changes in ocean circulation have affected the relevant areas for global ocean ventilation[21].

To explore these different aspects that link ASST and GAST to MOT, we evaluated oceanic and atmospheric temperature fields of